*Article*

# Electrochemical Stability Enhancement in Reactive Magnetron Sputtered VN Films upon Annealing Treatment

**Amine Achour [1], Mohammad Islam [2,*], Iftikhar Ahmad [2], Khalid Saeed [3] and Shahram Solaymani [4]**

[1] LISE Laboratory, Research Centre in Physics of Matter and Radiation (PMR), University of Namur, B-5000 Namur, Belgium; a_aminph@yahoo.fr

[2] Center of Excellence for Research in Engineering Materials, Deanship of Scientific Research, King Saud University, P.O. Box 800, Riyadh 11421, Saudi Arabia; ifahmad@ksu.edu.sa

[3] Department of Mechanical Engineering, King Saud University, P.O. Box 800, Riyadh 11421, Saudi Arabia; khaliduetp@gmail.com

[4] Young Researchers and Elite Club, West Tehran Branch, Islamic Azad University, Tehran, Iran; shahram22s2000@yahoo.com

* Correspondence: mohammad.islam@gmail.com or miqureshi@ksu.edu.sa; Tel.: +966-54-452-3909

check for updates

**Abstract:** Vanadium nitride (VN) thin films were produced via direct-current reactive magnetron sputtering technique followed by vacuum annealing. The treatment was carried out at different temperatures for any effect on their electrochemical (EC) stability, up to 10,000 charge–discharge cycles in 0.5 M $K_2SO_4$ solution. The film surface chemistry was investigated by using X-ray photoelectron spectroscope (XPS) and cyclic voltammetry (CV) techniques. For the as-deposited film, the oxide layer formed on the VN surface was unstable upon $K_2SO_4$ immersion treatment, along with ~23% reduction in the EC capacitance. Vacuum annealing under optimized conditions, however, made the oxide layer stable with almost no capacitance loss upon cycling for up to 10,000 cycles. Annealing treatment of the VN films makes them a potential candidate for long-term use in electrochemical capacitors.

## 1. Introduction

Owing to their high density and melting point, superior hardness, excellent electronic conductivity and high specific capacitance, vanadium nitride (VN) thin films offer strong potential for application in electrochemical capacitors (ECs) [1,2]. In this context, the hybrid nanostructures of VN films and carbon nanotubes have been reported to exhibit high volume capacitance, volume energy and power density [3]. Also, VN in nanocrystalline form demonstrated gravimetric capacitance of ~1300 $F \cdot g^{-1}$, due to successive, fast, and reversible redox reactions involving surface oxide groups and $OH^-$ ions from the electrolyte [4]. One of the major disadvantages associated with the use of VN, however, is its susceptibility to degradation that inhibits its practical application. It has been shown that cycling VN in KOH electrolyte leads to the degradation of the surface oxide layers that form at the surface of VN, and thus the capacitance decay over cycling [4]. Several factors, including film attributes such as crystallite size, morphology, surface oxide layer, etc., and EC test conditions; material loading, electrolyte concentration, and potential window, to name a few, influence the EC performance [5].

Both pure and nanocomposite VN films have been extensively explored for both structural [6,7] and functional applications [8–12]. The VN films exhibit pseudocapacitive behaviors through electric double-layer formation in the presence of $OH^-$ ions. Using N-doped carbon nanosheets/VN

nanoparticles hybrid composition as the electrode, high specific capacitance with about 60% retention after 5000 cycles was reported [11]. Another study reported a reduction in areal capacitance by ~80% within first 100 cycles, when tested for 1000 cycles in 1 M KOH solution [2]. Although cycle life stability is generally assessed in KOH electrolyte solution, it is also performed in mild $K_2SO_4$ solution due to the relatively slow rate of decay in the EC capacitance value [13,14]. We recently reported the electrochemical properties of VN/CNT hybrid nanostructures for micro-capacitors, using potassium sulphate ($K_2SO_4$) electrolyte [13]. Furthermore, we suggested the preservation of the surface oxide layer for enhanced VN film stability during cycling. In this work, we demonstrate from X-ray photoelectron spectroscope (XPS) analysis that VN film annealing under certain conditions can preserve the surface oxide layer, thus enhancing the cycling life stability in 0.5 M $K_2SO_4$ electrolyte. Such finding have implications in the design of stable VN thin film based materials for use in ECs.

## 2. Experimental Procedure

Direct-current (DC) plasma reactive magnetron sputtering technique was employed to produce VN films over silicon (100) substrates. The system consisted of a magnetron sputtering gun in a stainless steel chamber in which a base pressure of $<10^{-5}$ Pa was obtained using a turbo-molecular pump. Pure argon and nitrogen with 99.99% purity were used as sputtering and reactive gases, respectively. The target was a vanadium metal of $\geq$99.9% purity. The reactive sputtering was carried out without intentional substrate heating at a pressure of 0.32 Pa. The total gas flux rate during deposition was maintained at a constant value of 40 sccm, while the flow rate for reactive $N_2$ gas was fixed at 35%. The power density and deposition time were kept at 12.7 W/cm$^2$ and 3 hr, respectively. From these deposition conditions, the VN films with an average thickness value of ~690 nm were obtained, as estimated from scanning electron microscope (SEM) examination of the film cross-sections. The as-deposited VN film is referred to as $V_o$.

The films were then annealed in the same chamber at different temperatures for 2 h. The pressure inside the chamber during annealing was of the order of $5.5 \times 10^{-3}$ Pa. Due to low pressure during annealing, excessive oxidation of the films may be ruled out. The samples annealed at 400, 600, and 800 °C temperature were designated as $V_1$, $V_2$, and $V_3$, respectively.

The electrochemical measurements were performed in 0.5 M $K_2SO_4$ (Alfa Aesar, Ward Hill, MA, USA, 99.99%) electrolyte solution. A conventional cell with 3-electrode configuration was used in a VMP 3 multi potentiostat galvanostat (BioLogic, Seyssinet-Pariset, France) that was coupled with the EC-Lab software® V11.10.

The samples were examined under an SEM (JSM7600F; JEOL, Tokyo, Japan) by operating at 5 kV accelerating voltage and 4.5 mm working distance. The X-ray diffraction (XRD) patterns were obtained from Siemens D5000 diffractometer (Siemens, Berlin, Germany) with Bragg Brentano configuration and monochromatic CuKα1 radiation. The film surface chemistry was investigated ex situ using an X-ray photoelectron spectroscope (XPS) (Kratos Axis Ultra, Kratos Analytical Ltd, Manchester, UK). The Al Kα radiation (1486.6 eV) at 20 eV pass energy and 0.9 eV energy resolution was employed to record high-resolution spectra. As a reference, the C 1s line of 284.4 eV was used for any correction in the shift in binding energies. The XPS spectra in the V 2p core-level regions were analyzed through a peak-fitting procedure, using a Shirley background.

## 3. Results and Discussion

### 3.1. Morphology and Composition

The SEM microstructures of the as-deposited VN electrode surface and the cross-section are shown in Figure 1. As evident in Figure 1a, the film surface was observed to be comprised of nanostructured grains with a pyramid-like morphology and an average grain size of ~37 nm. Due to this specific granular morphology, the film appeared to exhibit a very high surface area, which could cause an enhancement in the specific capacitance. Also, the high film surface roughness (not measured

quantitatively) implied the presence of surface pores, as evident from a few dark, depressed spots between grains. The porosity level is nevertheless very low, and is believed to be at the film surface only. Microstructural examination of the film cross-section revealed dense, columnar growth with very little porosity. From the cross-sectional microstructure (Figure 1b), the film thickness was estimated to be ~690 nm, with a corresponding growth rate of 230 nm/hr. Although not shown here, the $V_1$, $V_2$, and $V_3$ films did not undergo any noticeable change in surface morphology upon vacuum thermal annealing at temperatures of 400 to 800 °C.
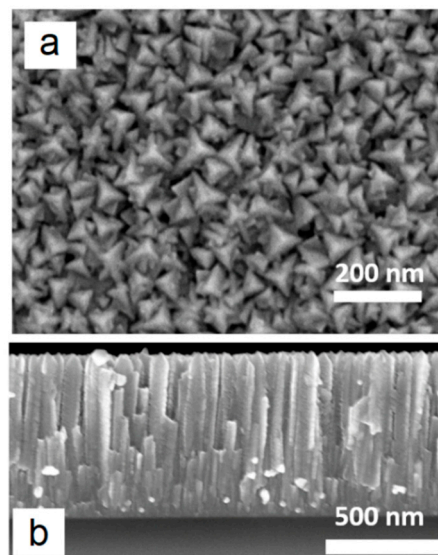


**Figure 1.** SEM micrographs of the as-prepared vanadium nitride (VN) film: (**a**) Surface microstructure, and (**b**) Cross-sectional view.

The XRD patterns of the as-deposited and vacuum annealed VN films are presented in Figure 2. All the samples exhibited one peak located at ~37.8° that was indexed to be (111) plane of the face-centered cubic VN (JCPDS No. 35-0768) [15]. The peak is broad, indicative of the small size of the individual crystallites in the deposited film. Upon thermal treatment, a small shift towards a greater diffraction angle was noticed, which may be attributed to stress relaxation, with consequent reduction in the lattice constant. The fcc δ-VN phase formation under the prevailing conditions of power density (12.7 W·cm$^{-2}$) and nitrogen gas flow (14 sccm) as well as the resulting film growth rate (3.83 nm·min$^{-1}$) confirm the findings reported earlier [16,17].
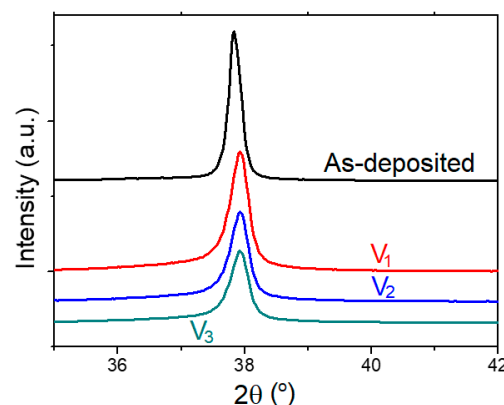


**Figure 2.** XRD patterns of the as-deposited and vacuum-annealed VN films.

### 3.2. Cyclic Voltammetry and XPS Analysis of as-Deposited VN Film

For the as-deposited VN film ($V_o$), cyclic voltammetry experiments were performed at a 200 mV·s$^{-1}$ scan rate. The cyclic voltammograms of the VN films after 3 and 10,000 consecutive cycles are showcased in Figure 3. Upon repeated charge–discharge cycling, a decay in the electrochemical capacitance by ~23% was observed. It is noteworthy that the electrochemical treatment did not induce any modification in the film surface morphology or structure after cycling.
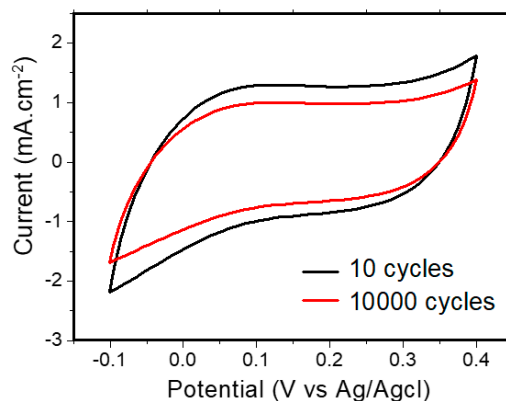


**Figure 3.** Cycling voltammograms of the as-deposited VN film in $K_2SO_4$ solution at a 200 mV·s$^{-1}$ scan rate after 3 and 10,000 cycles.

XPS analysis was performed to determine any changes in film surface chemistry before and after EC cycling. For the as-deposited VN film (no thermal treatment), the chemical nature of the film surface is showcased in Figure 4 through V 2p and N 1s high resolution XPS spectra before and after EC cycling. The V 2p$_{3/2}$ spectral regime revealed presence of four peaks at binding energies (BE) of 513.4, 514.2, 515.5, and 517.1 eV. While the first peak is associated with VN, the latter three may be assigned to $V_2O_3$, $VO_2$ and $V_2O_5$ compositions, respectively [18,19]. It is noteworthy that, like most transition metal nitrides, surface oxidation of the VN film occurred upon air exposure and aging. It was observed that in the V 2p spectrum (Figure 4a), the intensity of the $V_2O_5$ peak was reduced after cycling. On the other hand, the peak intensity for $VO_xN_y$ remained unchanged after cycling, as revealed by high resolution spectra of the N 1s peaks (Figure 4b). The electrochemical charge–discharge cycling of the as-deposited VN film, therefore, causes deterioration of the oxide layer over the VN film surface, thus inducing a drop in the capacitance, as noticed in the cyclic voltammetry results (Figure 3).
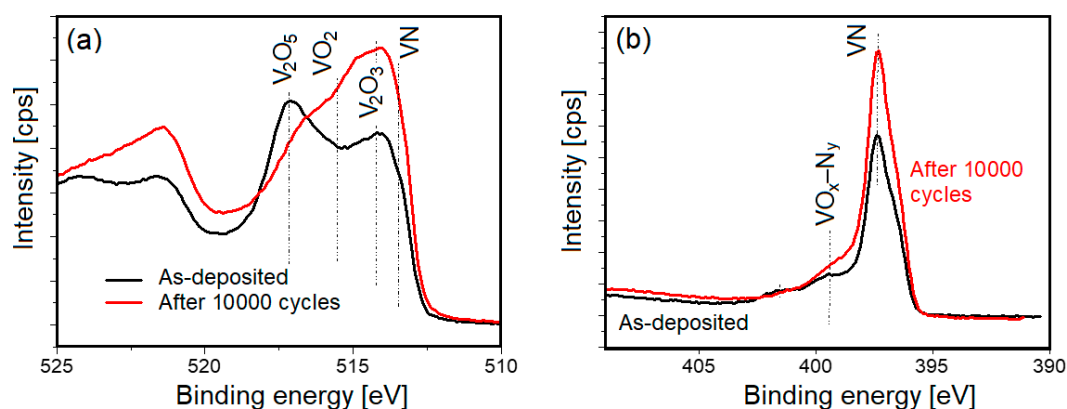


**Figure 4.** X-ray photoelectron spectroscope (XPS) data of the as-deposited VN film before and after 10,000 charge-discharge cycles: (**a**) Core level V 2p spectra, and (**b**) Core level N 1s spectra.

### 3.3. Effect of Vacuum Annealing: XPS Analysis

The high resolution XPS V 2p spectra of the as-deposited as well as thermally treated VN films are represented in Figure 5. Before the EC charge/discharge cycling, the surface chemistry of the vacuum annealed VN films was different from that of as-produced film, in the sense that 600 and 800 °C thermal treatments promoted a slightly higher degree of surface oxide layer formation. This may be attributed to the partial oxidation of the film surface at high temperatures, even under vacuum [20]. Among the vacuum-annealed VN films, only $V_1$ sample (annealed at 400 °C) was noticed to undergo oxide degradation after 10,000 EC cycles, as evident from comparison of the XPS spectra (Figure 5a). Quite interestingly, however, the oxide content on the VN film surfaces in the case of $V_2$ and $V_3$ films (annealed at 600 and 800 °C) did not decrease after prolonged cycling, as demonstrated in Figure 5b,c.
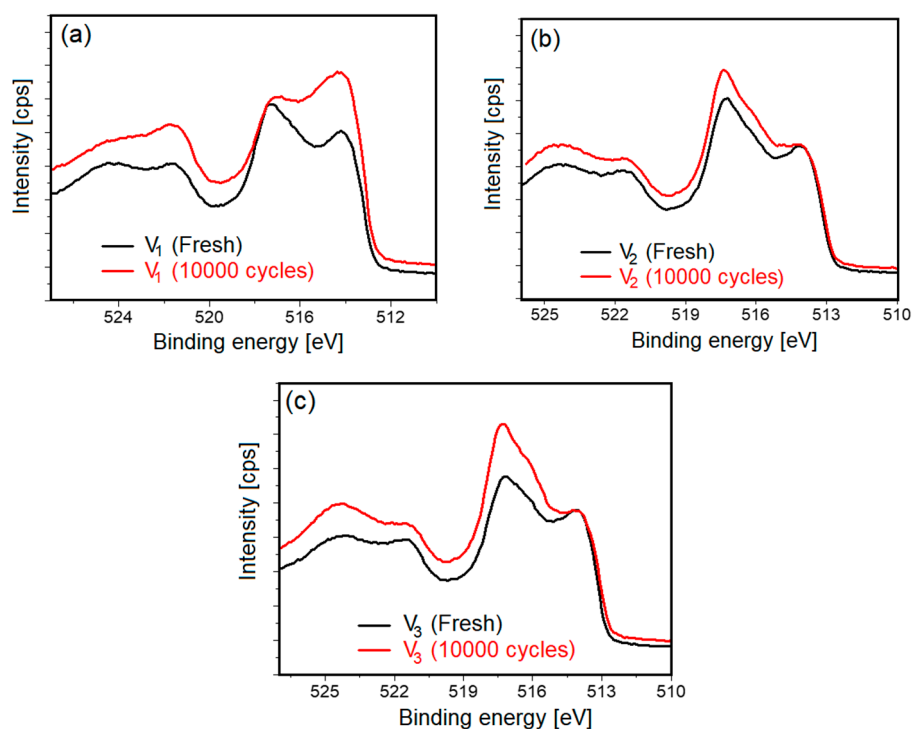


**Figure 5.** Comparison of the XPS core level V 2p spectra for the annealed VN films initially and after 10000 EC cycles: (**a**) $V_1$ sample, (**b**) $V_2$ sample, and (**c**) $V_3$ sample.

After EC charge/discharge tests for up to 10,000 cycles, the areal capacitance was plotted against the number of cycles, as shown in Figure 6a. For the $V_2$ and $V_3$ samples i.e., the VN films annealed at 600 and 800 °C, there was no deterioration in the areal capacitance level. Moreover, the specific capacitance was observed to be greater for the vacuum-annealed films, presumably because of an increase in the amount of oxide layer at the VN film surface. These findings indicate that vacuum annealing treatment leads to stabilization of the oxide surface layer. Factors such as formation of a thicker oxide layer, or crystallization of the oxide surface layer or both, might have been responsible for this behavior. The XPS V 2p core level spectra of the annealed VN films were recorded and deconvoluted to investigate the bonding characteristics of vanadium with oxygen and nitrogen, as presented in Figure 6b–d. The atomic percent of vanadium, bonded as $V_2O_3$, $VO_2$, and $V_2O_5$ compositions, are given as an inset in each case. Among the three samples examined, the presence of $V_2O_5$ and $V_2O_3$ phases was found to be maximized in case of sample $V_2$ (vacuum-annealed at 600 °C). Although the relative content of the $VO_2$ phase remained almost the same in all the films, there was an associated reduction in the VN phase content upon vacuum annealing. These observations signify the importance of annealing conditions towards any improvement in the electrochemical properties. In addition, the correlation between the capacitance improvement and the surface chemistry of the VN

films may offer an insight into the influence of the $V_yO_x$ composition on the capacitance behavior of the VN electrodes.
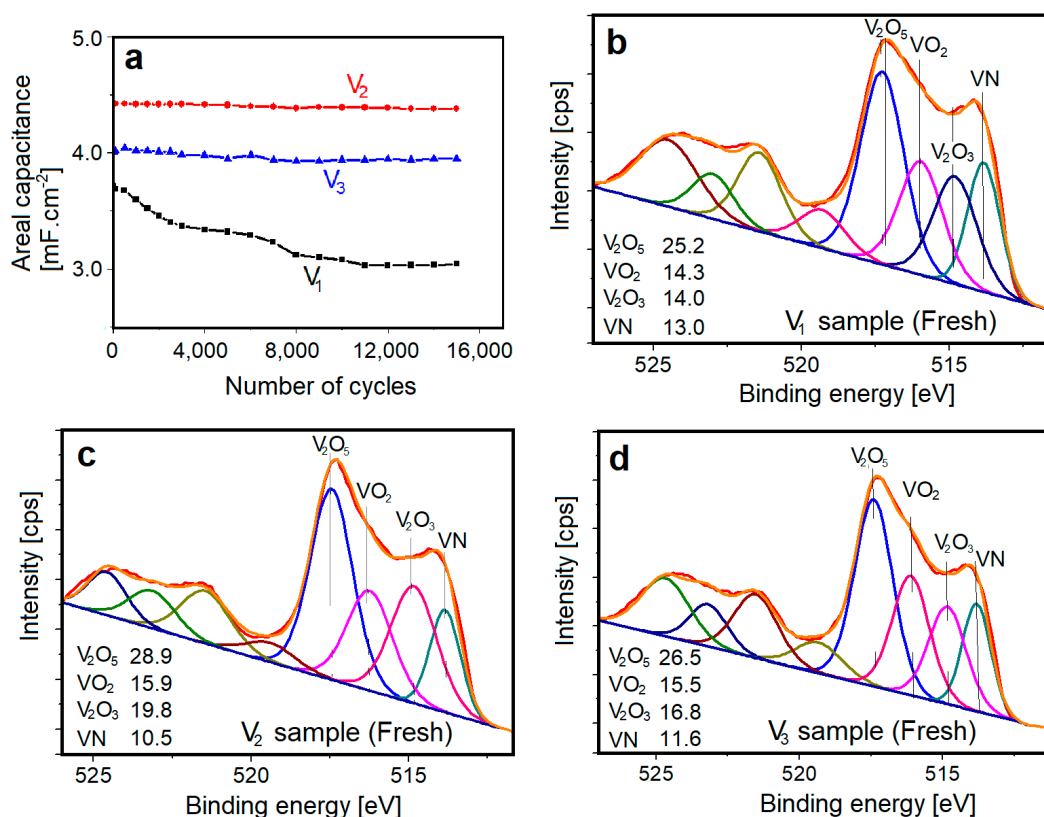


**Figure 6.** Cycling stability of the annealed VN film at 200 mV·s$^{-1}$ scan rate, and (**b–d**) XPS V 2p core level deconvoluted spectra of the annealed VN films: (**b**) $V_1$ sample, (**c**) $V_2$ sample, and (**d**) $V_3$ sample.

## 4. Conclusions

Nanocrystalline VN films were produced via DC-plasma reactive magnetron sputtering followed by thermal treatment under a vacuum at 400, 600, and 800 °C. For the as-deposited and 400 °C annealed VN films, the topmost surface oxide layer was found to degrade upon treatment in $K_2SO_4$ electrolyte solution. This was confirmed from XPS analysis besides a ~23% capacitance loss in the case of the as-deposited VN film after 10,000 cycles. Vacuum annealing of the VN films at 600 and 800 °C led to an enhancement in electrochemical cycling stability, with an almost 100% capacitance retention, even after 10,000 cycles. Such an improvement in EC properties is speculated to originate from VN film crystallization or a thickness increase in the surface oxide layer, or both. From this finding, VN-based electrode materials may be developed with superior VN cycling stability in electrochemical energy devices.

**Author Contributions:** A.A. and M.I. conceived the idea and designed the experimentation scheme; A.A., K.S., and I.A. performed the experiments; M.I. and S.S. carried out data analysis; A.A. and M.I. prepared the original manuscript draft with input from other co-authors. M.I. was responsible for acquisition of funding for this research.

**Conflicts of Interest:** The authors declare no conflict of interest.

## References

1.  Eustache, E.; Frappier, R.; Porto, R.L.; Bouhtiyya, S.; Pierson, J.F.; Brousse, T. Asymmetric electrochemical capacitor microdevice designed with vanadium nitride and nickel oxide thin film electrodes. *Electrochem. Commun.* **2013**, *28*, 104–106. [CrossRef]
2.  Liu, X.; Lu, H.; He, M.; Jin, K.; Yang, G.; Ni, H.; Zhao, K. Epitaxial growth of vanadium nitride thin films by laser molecule beam epitaxy. *Mater. Lett.* **2014**, *123*, 38–40. [CrossRef]
3.  Xiao, X.; Peng, X.; Jin, H.; Li, T.; Zhang, C.; Gao, B.; Hu, B.; Huo, K.; Zhou, J. Freestanding mesoporous VN/CNT hybrid electrodes for flexible all-solid-state supercapacitors. *Adv. Mater.* **2013**, *25*, 5091–5097. [CrossRef] [PubMed]
4.  Choi, D.; Blomgren, G.E.; Kumta, P.N. Fast and reversible surface redox reaction in nanocrystalline vanadium nitride supercapacitors. *Adv. Mater.* **2006**, *18*, 1178–1182. [CrossRef]
5.  Shu, D.; Lv, C.; Cheng, F.; He, C.; Yang, K.; Nan, J.; Long, L. Enhanced capacitance and rate capability of nanocrystalline VN as electrode materials for supercapacitors. *Int. J. Electrochem. Sci.* **2013**, *8*, 1209–1225.
6.  Fu, T.; Peng, X.; Wan, C.; Lin, Z.; Chen, X.; Hu, N.; Wang, Z. Molecular dynamics simulation of plasticity in VN(001) crystals under nanoindentation with a spherical indenter. *Appl. Surf. Sci.* **2017**, *392*, 942–949. [CrossRef]
7.  Sowa, M.J.; Ju, L.; Kozen, A.C.; Strandwitz, N.C.; Zeng, G.; Babuska, T.F.; Hsain, Z.; Krick, B.A. Plasma-enhanced atomic layer deposition of titanium vanadium nitride. *J. Vac. Sci. Technol. A* **2018**, *36*, 06A103. [CrossRef]
8.  Yan, Y.; Li, B.; Guo, W.; Pang, H.; Xue, H. Vanadium based materials as electrode materials for high performance supercapacitors. *J. Power Sources* **2016**, *329*, 148–169. [CrossRef]
9.  Zhu, L.; Li, C.; Ren, W.; Qin, M.; Xu, L. Multifunctional vanadium nitride@N-doped carbon composites for kinetically enhanced lithium–sulfur batteries. *New J. Chem.* **2018**, *42*, 5109–5116. [CrossRef]
10. Wu, Y.; Ran, F. Vanadium nitride quantum dot/nitrogen-doped microporous carbon nanofibers electrode for high-performance supercapacitors. *J. Power Sources* **2017**, *344*, 1–10. [CrossRef]
11. Tan, Y.; Liu, Y.; Tang, Z.; Wang, Z.; Kong, L.; Kang, L.; Liu, Z.; Ran, F. Concise N-doped carbon nanosheets/vanadium nitride nanoparticles materials via intercalative polymerization for supercapacitors. *Sci. Rep.* **2018**, *8*, 2915. [CrossRef] [PubMed]
12. Guo, J.; Zhang, Q.; Sun, J.; Li, C.; Zhao, J.; Zhou, Z.; He, B.; Wang, X.; Man, P.; Li, Q.; et al. Direct growth of vanadium nitride nanosheets on carbon nanotube fibers as novel negative electrodes for high-energy-density wearable fiber-shaped asymmetric supercapacitors. *J. Power Sources.* **2018**, *382*, 122–127. [CrossRef]
13. Ouldhamadouche, N.; Achour, A.; Lucio-Porto, R.; Islam, M.; Solaymani, S.; Arman, A.; Ahmadpourian, A.; Achour, H.; Le Brizoual, L.; Djouadi, M.A.; et al. Electrodes based on nano-tree-like vanadium nitride and carbon nanotubes for micro-supercapacitors. *J. Mater. Sci. Technol.* **2018**, *34*, 976–982. [CrossRef]
14. Bondarchuk, O.; Morel, A.; Bélanger, D.; Goikolea, E.; Brousse, T.; Mysyk, R. Thin films of pure vanadium nitride: Evidence for anomalous nonfaradaic capacitance. *J. Power Sources* **2016**, *324*, 439–446. [CrossRef]
15. Hajihoseini, H.; Kateb, M.; Ingvarsson, S.; Gudmundsson, J.T. Effect of substrate bias on properties of HiPIMS deposited vanadium nitride films. *Thin Solid Films* **2018**, *663*, 126–130. [CrossRef]
16. Farges, G.; Beauprez, E.; Degout, D. Preparation and characterization of V–N films deposited by reactive triode magnetron sputtering. *Surf. Coat. Technol.* **1992**, *54–55*, 115–120.
17. Hajihoseini, H.; Gudmundsson, J.T. Vanadium and vanadium nitride thin films grown by high power impulse magnetron sputtering. *J. Phys. D Appl. Phys.* **2017**, *50*, 505302. [CrossRef]
18. Sun, Y.; Liu, K.; Miao, J.; Wang, Z.; Tian, B.; Zhang, L.; Li, Q.; Fan, S.; Jiang, K. Highly sensitive surface-enhanced Raman scattering substrate made from superaligned carbon nanotubes. *Nano Lett.* **2010**, *10*, 1747–1753. [CrossRef] [PubMed]
19. Boukhalfa, S.; Evanoff, K.; Yushin, G. Atomic layer deposition of vanadium oxide on carbon nanotubes for high-power supercapacitor electrodes. *Energy Environ. Sci.* **2012**, *5*, 6872–6879. [CrossRef]
20. Glaser, A.; Surnev, S.; Netzer, F.P.; Fateh, N.; Fontalvo, G.A.; Mitterer, C. Oxidation of vanadium nitride and titanium nitride coatings. *Surf. Sci.* **2007**, *601*, 1153–1159. [CrossRef]